

## Metastability and relaxation in tensile SiGe on Ge(001) virtual substrates

Jacopo Frigerio, Mario Lodari, Daniel Chrastina, Valeria Mondiali, Giovanni Isella, and Monica Bollani

Citation: *Journal of Applied Physics* **116**, 113507 (2014); doi: 10.1063/1.4896076

View online: <http://dx.doi.org/10.1063/1.4896076>

View Table of Contents: <http://scitation.aip.org/content/aip/journal/jap/116/11?ver=pdfcov>

Published by the [AIP Publishing](#)

---

### Articles you may be interested in

[Strain relaxation of metastable SiGe/Si: Investigation with two complementary X-ray techniques](#)

*J. Appl. Phys.* **111**, 063507 (2012); 10.1063/1.3694037

[Terrace grading of SiGe for high-quality virtual substrates](#)

*Appl. Phys. Lett.* **81**, 4775 (2002); 10.1063/1.1529308

[Loading effect in SiGe layers grown by dichlorosilane- and silane-based epitaxy](#)

*J. Appl. Phys.* **90**, 4805 (2001); 10.1063/1.1406541

[Effective compliant substrate for low-dislocation relaxed SiGe growth](#)

*Appl. Phys. Lett.* **78**, 1219 (2001); 10.1063/1.1351520

[Compliant effect of low-temperature Si buffer for SiGe growth](#)

*Appl. Phys. Lett.* **78**, 454 (2001); 10.1063/1.1337633

---



**HIDEN ANALYTICAL** Instruments for Advanced Science

 <p><b>Gas Analysis</b></p> <ul style="list-style-type: none"><li>dynamic measurement of reaction gas streams</li><li>catalysis and thermal analysis</li><li>molecular beam studies</li><li>dissolved species probes</li><li>fermentation, environmental and ecological studies</li></ul>	 <p><b>Surface Science</b></p> <ul style="list-style-type: none"><li>UHV TPD</li><li>SIMS</li><li>end point detection in ion beam etch</li><li>elemental imaging - surface mapping</li></ul>	 <p><b>Plasma Diagnostics</b></p> <ul style="list-style-type: none"><li>plasma source characterization</li><li>etch and deposition process reaction</li><li>kinetic studies</li><li>analysis of neutral and radical species</li></ul>	 <p><b>Vacuum Analysis</b></p> <ul style="list-style-type: none"><li>partial pressure measurement and control of process gases</li><li>reactive sputter process control</li><li>vacuum diagnostics</li><li>vacuum coating process monitoring</li></ul>
--	---	---	---

Contact Hiden Analytical for further details:  
[www.HidenAnalytical.com](http://www.HidenAnalytical.com)  
[info@hiden.co.uk](mailto:info@hiden.co.uk)  
**CLICK TO VIEW** our product catalogue

## Metastability and relaxation in tensile SiGe on Ge(001) virtual substrates

Jacopo Frigerio,<sup>1</sup> Mario Lodari,<sup>1</sup> Daniel Chrastina,<sup>1,a)</sup> Valeria Mondiali,<sup>1</sup> Giovanni Isella,<sup>1</sup> and Monica Bollani<sup>2</sup>

<sup>1</sup>L-NESS, Dipartimento di Fisica, Politecnico di Milano, Polo di Como, via Anzani 42, 22100 Como, Italy

<sup>2</sup>IFN-CNR, L-NESS, via Anzani 42, 22100 Como, Italy

(Received 27 June 2014; accepted 8 September 2014; published online 17 September 2014)

We systematically study the heteroepitaxy of SiGe alloys on Ge virtual substrates in order to understand strain relaxation processes and maximize the tensile strain in the SiGe layer. The degree of relaxation is measured by high-resolution x-ray diffraction, and surface morphology is characterized by atomic force microscopy. The results are analyzed in terms of a numerical model, which considers dislocation nucleation, multiplication, thermally activated glide, and strain-dependent blocking. Relaxation is found to be sensitive to growth rate and substrate temperature as well as epilayer misfit and thickness, and growth parameters are found which allow a SiGe film with over 4 GPa of tensile stress to be obtained. © 2014 AIP Publishing LLC.

[<http://dx.doi.org/10.1063/1.4896076>]

### I. INTRODUCTION

Germanium is an indirect-gap semiconductor, with the valence band maximum at  $\Gamma$  and the conduction band minimum at L. However, a local minimum exists in the conduction band at  $\Gamma$ , which is only 140 meV above L at room temperature.<sup>2</sup> Tensile strain reduces this separation, and heavy n-type doping has been suggested as a way of filling the L-valley as a possible route towards optical gain,<sup>3,4</sup> but with the attendant disadvantage that heavy doping leads to an increase of the optical absorption and non-radiative recombination.<sup>5,6</sup>

The application of 2% biaxial tensile strain to a Ge(001) layer is expected to lower the direct gap below that of the indirect gap,<sup>7</sup> and a similar result is expected for 4%–5% uniaxial strain applied along [110].<sup>8</sup> A direct-gap semiconductor which is fully compatible with Si-based technology would allow full integration of electronics and optoelectronics and represents a highly sought goal,<sup>9,10</sup> so various methods of inducing the required strain in Ge micro- and nano-structures are under investigation.<sup>11–19</sup> Ge microbridges featuring 3% uniaxial strain along [100] have demonstrated greatly enhanced photoluminescence efficiency,<sup>20</sup> and even higher strain has been observed in smaller bridges.<sup>21</sup>

It has been shown that patterning of compressively strained SiGe alloys on Si(001) substrates leads to the transfer of compressive strain into the substrate.<sup>22,23</sup> An analogous process should therefore be feasible in which patterned tensile SiGe alloys on Ge(001) substrates induce tensile strain in the Ge.<sup>19</sup>

Relaxation and metastability have been extensively studied in compressive SiGe alloys on Si(001).<sup>24–31</sup> The equilibrium critical thickness for high lattice parameter mismatch (more than 2%) can be as small as 4 nm,<sup>32</sup> but under certain conditions (i.e., fast epitaxy at relatively low temperatures) thicker metastable films can be realized in which the

nucleation of dislocations can be delayed.<sup>33</sup> However, studies of tensile strain in the SiGe system have mainly been limited to Si on Si-rich SiGe virtual substrates (VSs),<sup>34–39</sup> and reverse-graded buffers.<sup>40–43</sup> Capellini *et al.* studied the relaxation of a Si<sub>0.22</sub>Ge<sub>0.78</sub> layer on a Ge VS (as compared to directly on Si) following a similar work by Demczyk *et al.*<sup>44,45</sup> In this work, we present a systematic study of the conditions required in order to obtain tensile Si<sub>1-x</sub>Ge<sub>x</sub> films ( $0.4 \leq x \leq 0.6$ ) on Ge(001) VSs, to use as stressors for the underlying Ge,<sup>19</sup> and interpret the experimental data by means of a model based on dislocation nucleation, thermally activated glide, and blocking.

### II. SAMPLE GROWTH

Tensile SiGe layers were obtained by low-energy plasma-enhanced chemical vapor deposition (LEPECVD), with a method similar to that described in Refs. 22 and 23, starting from HF-dipped Si(0 0 1) 4-in. wafers. A 1  $\mu$ m Ge layer was deposited at 500 °C at a growth rate of 4.3 nm s<sup>-1</sup>, and then annealed *in-situ* over six cycles between 600 and 800 °C in order to reduce the threading dislocation density (which leaves a small amount of thermal tensile strain,  $\varepsilon_{\parallel} \sim 0.12\%–0.16\%$ , in the Ge layer).<sup>46</sup> The resulting Ge/Si(001) layer forms a VS for the subsequent growth of a thin (20–100 nm) Si<sub>1-x</sub>Ge<sub>x</sub> layer. The composition  $x$  and relaxation  $\beta$  of both the Ge and Si<sub>1-x</sub>Ge<sub>x</sub> layers were measured by high-resolution x-ray diffraction, employing the (004) and grazing-incidence (224) Bragg peaks. In the case of fully strained Si<sub>1-x</sub>Ge<sub>x</sub> layers, fringes were visible along  $q_{\perp}$ , which confirmed the thickness of the Si<sub>1-x</sub>Ge<sub>x</sub> layer. Data are shown in Fig. 2. The uncertainty in the measurement of  $\beta$  mainly comes from peak broadening in the  $q_{\parallel}$  direction due to defects, and also broadening in the  $q_{\perp}$  direction due to the finite thickness of the layers.<sup>47</sup> The (224) reciprocal space map (RSM) of a sample featuring 40 nm of Si<sub>0.6</sub>Ge<sub>0.4</sub> grown at 500 °C is shown in Fig. 1(a). XRD data indicate that the SiGe layer is defective and partially relaxed.

<sup>a)</sup>Electronic mail: daniel.chrastina@polimi.it

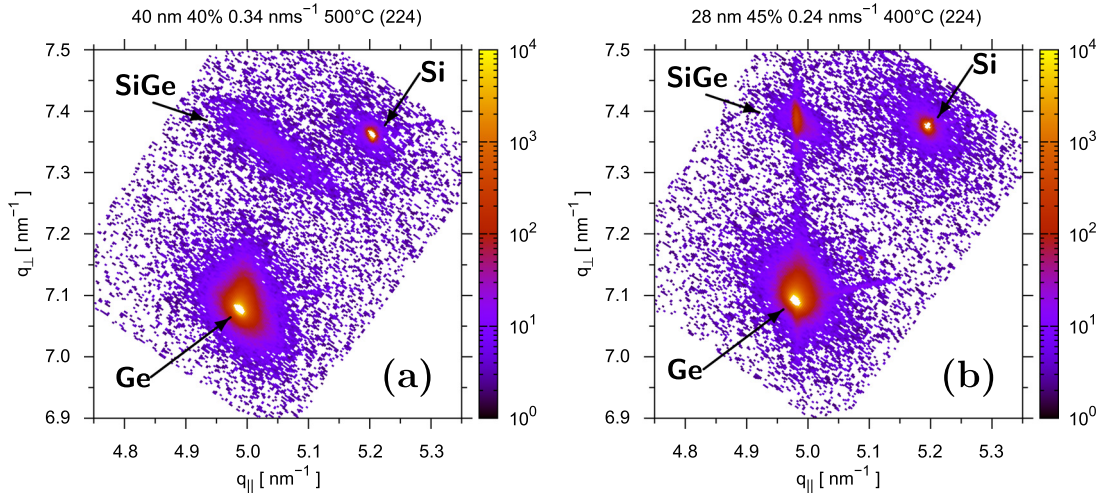


FIG. 1. XRD reciprocal space maps at the (224) reflection for (a) a 40 nm  $\text{Si}_{0.6}\text{Ge}_{0.4}$  film deposited epitaxially (at 500 °C and a growth rate of  $0.34 \text{ nms}^{-1}$ ) on a Ge VS, and (b) a 28 nm  $\text{Si}_{0.55}\text{Ge}_{0.45}$  film deposited epitaxially (at 400 °C and a growth rate of  $0.24 \text{ nms}^{-1}$ ) on a Ge VS. The intensity scale (in counts per second) has been limited in order to show the thin SiGe layer more clearly. In (a), the scattering vector of the SiGe peak is a shifted towards larger values of  $q_{\parallel}$  as compared to the Ge peak, indicating a relaxation of 34%. The SiGe peak is also broadened by defects associated with relaxation. However, in (b), the SiGe peak is aligned at the same  $q_{\parallel}$  as the Ge peak and is relatively narrow in the  $q_{\parallel}$  direction. Broadening and thickness fringes are visible in the  $q_{\perp}$  direction, which allow the film thickness to be confirmed and indicate that the SiGe film is fully strained.

In order to exploit strained SiGe layers for bandgap engineering through nanopatterning (Refs. 19, 22, and 23), it is essential to analyze the dynamics of tensile-strain relaxation. To this end, we have applied a model originally developed for compressively strained SiGe on Si. The effects of mismatch are not expected to be asymmetric for the considered misfits of 1%–2%.<sup>48</sup>

### III. RELAXATION MODEL

The model bases the rate of relaxation on the areal density of mobile threading dislocations  $N(t)$  and the dislocation velocity  $v(t)$ <sup>31,49</sup>

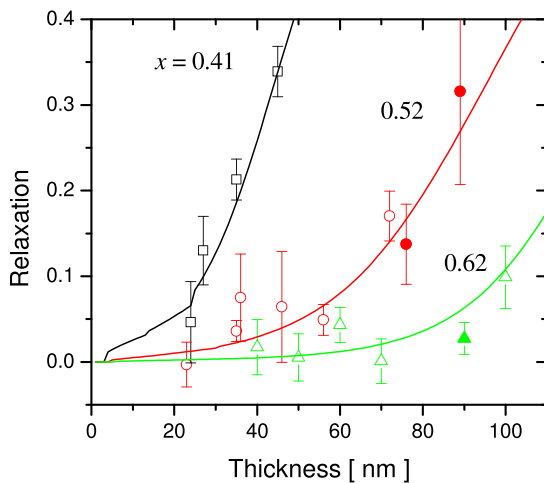


FIG. 2. Measured relaxation in  $\text{Si}_{1-x}\text{Ge}_x$  films deposited epitaxially on Ge VSs, for three different values of the nominal Ge content  $x$ . All  $\text{Si}_{1-x}\text{Ge}_x$  layers were grown at the same nominal substrate temperature of 500 °C and growth rate of  $0.34 \pm 0.02 \text{ nms}^{-1}$ . However, the data are scattered slightly around the lines calculated using the relaxation model, due to variations in the real growth rate and Ge content. (The Ge contents are within  $\pm 0.01$  of the values indicated on the graph apart from the 20 nm  $\text{Si}_{0.6}\text{Ge}_{0.4}$  sample in which  $x = 0.43$ ; filled symbols indicate sample growth rates of  $0.4\text{--}0.5 \text{ nms}^{-1}$ .)

$$\frac{d\beta}{dt} = \frac{b}{4f} N(t)v(t) \quad (1)$$

in which  $b = a(x)/\sqrt{2}$  is the Burger's vector for  $60^\circ$  dislocations in the  $\text{Si}_{1-x}\text{Ge}_x$  film with unstrained lattice parameter  $a(x)$ ,<sup>50</sup> and  $f = a_{\text{VS}}/a(x) - 1$  is the mismatch between the in-plane lattice parameter  $a_{\text{VS}}$  of the Ge VS and  $a(x)$ . The relaxation  $\beta$  of the tensile  $\text{Si}_{1-x}\text{Ge}_x$  film with in-plane lattice parameter  $a_{\parallel}$  on the Ge VS is defined as

$$\beta = \frac{a_{\parallel} - a_{\text{VS}}}{a(x) - a_{\text{VS}}}; \quad (2)$$

$v(t)$  depends on the excess stress  $\sigma$  and is thermally activated with a composition-dependent energy,  $E_A(x)$ , so that<sup>27</sup>

$$v(t) = BS\sigma \exp\left(\frac{-E_A(x)}{k_B T}\right) \quad (3)$$

in which the prefactor  $B$  is  $2.89 \times 10^{-3} \text{ sm}^2\text{kg}^{-1}$  and the Schmid factor  $S$  is  $1/\sqrt{6}$ .

An activation energy of  $E_A(x) = (2.156 - 0.7x) \text{ eV}$  is reported in the literature for compressively strained SiGe/Si,<sup>27</sup> which would give values of  $\sim 1.7\text{--}1.9 \text{ eV}$  in our case. However, some reports indicate that stress can reduce  $E_A$  as far as  $\sim 1.1 \text{ eV}$ .<sup>25,26</sup> Here, we do not attempt to consider the stress-dependence of  $E_A$  but note that the values we find ( $\sim 1.6 \text{ eV}$ ) are slightly reduced with respect to those which would be predicted for  $x \sim 0.6\text{--}0.4$  by the above equation.

The excess stress is given by<sup>31</sup>

$$\sigma = \frac{G \cos \psi}{1 - \nu} \times \left( 2 \cos \alpha (1 + \nu) |\varepsilon_{\parallel}| - \frac{b(1 - \cos^2 \alpha) \ln(h/b)}{4\pi h} \right) \quad (4)$$

for films of thickness  $h$  above the Matthews–Blakeslee equilibrium critical thickness  $h_c$ <sup>32</sup>

TABLE I. Fixed material growth parameters used in the relaxation model.

Parameter	Value	Meaning
$r_G$	0.3 nms <sup>-1</sup>	Growth rate
$T_g$	500 °C	Growth temperature
$r_c$	1.0 Ks <sup>-1</sup>	Cooling rate

$$h_c = \frac{b}{f} \left( \frac{1 - \nu/4}{4\pi(1 + \nu)} \right) \left[ \ln \left( \frac{h_c}{b} \right) + 1 \right]. \quad (5)$$

$\alpha = 60^\circ$  and  $\cos \psi = \sqrt{2/3}$ ,  $G \equiv c_{44}$  is the shear modulus and  $\nu = 1/(1 + c_{11}/c_{12})$  is the Poisson ratio, both found by linear interpolation of the stiffness constants between the values for pure Si and pure Ge.<sup>51</sup> The in-plane strain  $\varepsilon_{||}$  is related to  $f$  and  $\beta$  via  $\varepsilon_{||} = f(1 - \beta)$ .

The number of mobile dislocations increases due to nucleation and multiplication processes and decreases due to blocking and annihilation<sup>31,49</sup>

$$J_{nucl} = J_0 \exp \left( \frac{-E_T}{k_B T |\varepsilon_{||}|} \right), \quad (6)$$

$$J_{mult} = \frac{\beta N(t) v(t)}{bf} P_{mult}, \quad (7)$$

$$J_{block} = k_{block} N(t)^2, \quad (8)$$

$$\frac{dN}{dt} = J_{nucl} + J_{mult} - J_{block}. \quad (9)$$

The activation energy for nucleation  $E_T = 26$  meV, and  $P_{mult}$  increases at the thicknesses corresponding to activation of spiral and Frank-Read sources<sup>29</sup>

$$P_{mult} = \begin{cases} 0 & \text{for } h < h_c + h_p, \\ P_0 & \text{for } h_c + h_p < h < h_c + 2h_p, \\ 2P_0 & \text{for } h > h_c + 2h_p, \end{cases} \quad (10)$$

with

$$h_p = \frac{b}{f} \left( \frac{2 + \nu}{4\pi(1 - \nu)} \right) \left[ \ln \left( 4\sqrt{6} \frac{h_p}{b} \right) + \frac{\nu - 2}{\nu + 2} \right]. \quad (11)$$

While the  $J_{block}$  term may be effective in considering the strong blocking caused by stacking faults, which are

TABLE II. Variable model parameters used to fit the relaxation model to the data in Fig. 2.  $N_0$  is rather higher than is typically considered for the relaxation of SiGe on Si substrates, since the Ge VS is much more defective than a Si wafer even after annealing cycles. This value also incorporates the possibility of grown-in defects, especially point defects, which are expected to be more numerous for faster growth at lower temperatures.<sup>1</sup> The value of  $E_T$  is taken directly from Ref. 31 but  $J_0$  is much higher, and  $k_{block}$  is smaller.

Parameter	Value	Meaning
$N_0$	10 <sup>5</sup> cm <sup>-2</sup>	Initial dislocation density
$J_0$	1.5 × 10 <sup>11</sup> cm <sup>-2</sup> s <sup>-1</sup>	Nucleation prefactor (Eq. (7))
$E_T$	26 meV	Nucleation activation (Eq. (7))
$P_0$	10 <sup>-6</sup>	Multiplication (Eq. (10))
$k_{block}$	10 <sup>-6</sup> cm <sup>2</sup> s <sup>-1</sup>	Blocking rate (Eq. (9))

TABLE III. Activation energies used to fit the relaxation model to the data in Fig. 2.

Ge content	$E_A$ [eV]
0.40	1.593
0.50	1.615
0.60	1.615

characteristic of the relaxation of tensile (but not compressive) SiGe,<sup>52,53</sup> we also consider that the strain field of existing dislocations reduces the effective film thickness  $h^*$  which mobile dislocations can glide through,<sup>54,55</sup> so we use

$$\frac{h^*}{h} \simeq 1 - \left( \frac{0.09}{[h/b]\varepsilon_{||}} \right) \quad (12)$$

as an approximation to the numerical calculation presented in Fig. 7 of Ref. 55, and use  $h^*$  in Eq. (4) instead of  $h$ . This has the effect of stabilizing partially relaxed films, which would otherwise be predicted to quickly reach  $\sim 90\%$  relaxation after a short annealing process at the growth temperature (a sample featuring a 60 nm layer of Si<sub>0.5</sub>Ge<sub>0.5</sub>, which was 11% relaxed after growth, did not relax further following annealing for 100 s at 500 °C, and only reached 34% relaxation following annealing at 650 °C at 600 s).

#### IV. RESULTS

The parameters used to generate the curves shown in Fig. 2 are shown in Tables I–III. The parameters in Table I are considered fixed, but interaction between the parameters in Table II means it is probably difficult to extract physical insight from their values.<sup>31</sup> The model is, however, very sensitive to the values of  $E_A$  shown in Table III.  $E_A$  decreases

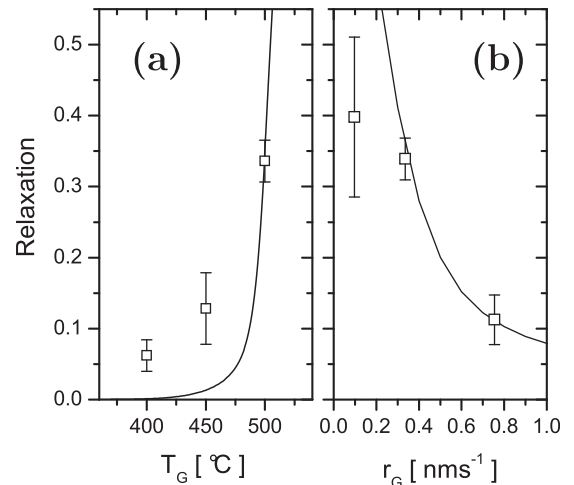


FIG. 3. Measured relaxation in 45 nm Si<sub>0.6</sub>Ge<sub>0.4</sub> films as a function of (a) growth temperature  $T_G$  (at  $\sim 0.34$  nms<sup>-1</sup>) and (b) growth rate  $r_G$  (at 500 °C). The model predicts a greater degree of relaxation for the sample grown at the lowest rate, but as can be seen in the AFM image of Fig. 4(a), this sample is probably very defective, leading to an even stronger degree of blocking than that included in the model. The model predicts also that fully strained films should be readily obtained on slightly lowering the growth temperature below 500 °C. The observed slight relaxation of films grown at lower temperature may be due to an increased density of grown-in point defects.<sup>1</sup>

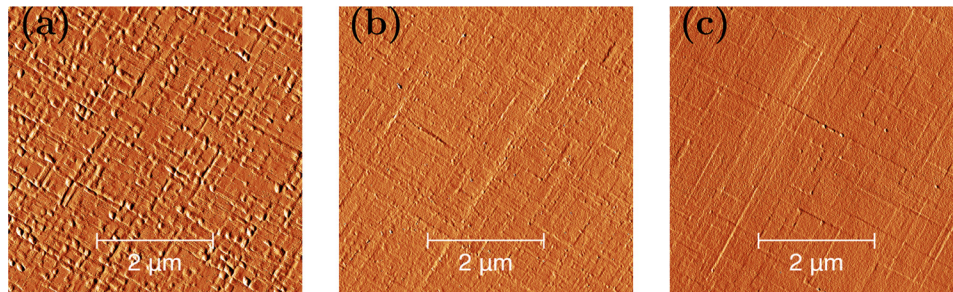


FIG. 4. Tapping amplitude AFM images, which give a qualitative indication of the sample topography, showing crosshatch lines along  $[110]$  and  $[\bar{1}\bar{1}0]$  directions, as is typical in the SiGe system. The samples feature 40 nm of  $\text{Si}_{0.6}\text{Ge}_{0.4}$  grown at  $500^\circ\text{C}$ . The growth rates are, from left to right, (a)  $0.10$ , (b)  $0.34$ , and (c)  $0.75 \text{ nm s}^{-1}$ . The rms roughnesses are, from left to right, (a)  $1.20$ , (b)  $0.26$ , and (c)  $0.22 \text{ nm}$ . The relaxation of these samples is shown in Fig. 3.

with increasing Ge content  $x$ ,<sup>27</sup> but is also expected to decrease with increasing stress.<sup>25,26</sup> For the  $\text{Si}_{1-x}\text{Ge}_x/\text{Si}$  system, these two effects work in the same direction; while for  $\text{Si}_{1-x}\text{Ge}_x/\text{Ge}$ , the two effects counteract each other, which may explain why we find  $E_A$  to be roughly constant.

The modeled relaxation is sensitive to growth rate, and this is explored in Fig. 3(b). Higher growth rate leads to a lower degree of relaxation, since the film has less time to relax at the growth temperature. Atomic force microscopy (AFM) images of these samples are shown in Fig. 4. The sample grown at the lowest rate is probably very defective, leading to a strong degree of blocking. Additionally, the grown-in point defect density may be lower at a lower growth rate, leading to slower nucleation and multiplication.<sup>1</sup>

The LEPECVD growth technique gives an inhomogeneous thickness distribution across a 100 mm wafer<sup>56</sup> from the nominal thickness close to the center of the wafer to about 60% of the nominal thickness at the edge. This corresponds to material grown at different rates but for the same growth time and temperature. The sample featured in Fig. 3 at a rate of  $0.34 \text{ nm s}^{-1}$  is 45 nm thick close to the center but only 25 nm thick near the edge (all for the same total growth time

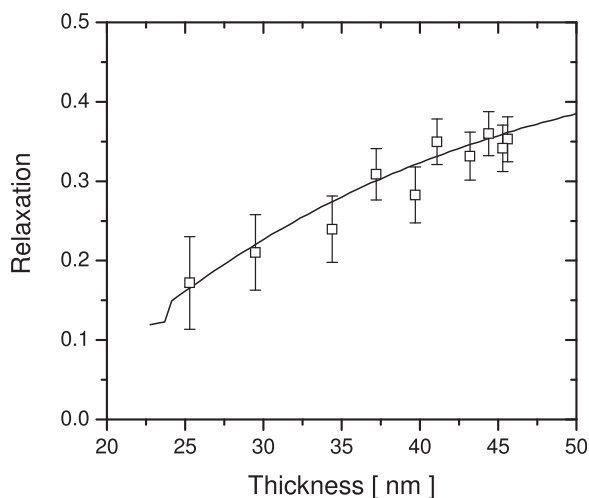


FIG. 5. Analysis of the variation of relaxation across a single wafer of nominally 45 nm  $\text{Si}_{0.60}\text{Ge}_{0.40}$  grown at  $500^\circ\text{C}$ . The higher plasma density towards the center of the wafer means that LEPECVD growth is faster and the resulting material is thicker in the center of the wafer as compared to the edge. This has been modeled by considering a variable growth rate but constant growth time. The effect of increased thickness, leading to increased relaxation, dominates over the effect of slower growth giving more time for relaxation to develop.

of 134 s) and the variation of relaxation can be modeled as shown in Fig. 5.

A further suggestion that  $N_0$  may depend on growth temperature is given by the relaxation behaviour of samples grown at lower temperature, as shown in Fig. 3(a): the samples relax more than is predicted. In addition, a model in which  $E_A$  decreases with stress may help to explain the onset of relaxation in samples grown at lower temperatures, but the present data set does not yet justify the increase in complexity of the model.

The present model does, however, suggest the possibility of obtaining SiGe films with a high degree of tensile strain by lowering the growth temperature and choosing a careful balance of Ge content and film thickness, and a film with 28 nm of  $\text{Si}_{0.55}\text{Ge}_{0.45}$  grown at  $400^\circ\text{C}$  is fully strained, as shown in Fig. 1(b). The stress in this film is around 4 GPa. Comprehensive finite-element model simulations carried out in Ref. 19 show that such material should be optimal for strain-transfer via nanopatterning, as has recently been demonstrated for SiGe on Si.<sup>22,23</sup>

## V. CONCLUSIONS

In conclusion, in this paper, we have experimentally and theoretically investigated the metastability and relaxation in thin SiGe films grown on Ge(001) virtual substrates. We have characterized the dynamics of plastic relaxation as a function of the growth rate and the substrate temperature in order to obtain tensile  $\text{Si}_{1-x}\text{Ge}_x$  films ( $0.4 < x < 0.6$ ) on Ge VS. Compared to calculations of equilibrium critical thickness, using the LEPECVD system, we have grown thicker metastable films in a manner analogous to the growth of metastable compressive SiGe layers directly on Si. A SiGe film with 4 GPa of tensile stress has been obtained, suitable for eventual nanopatterning into stressors in order to induce tensile strain in the Ge VS.

## ACKNOWLEDGMENTS

We acknowledge the Cariplo Foundation (within the grant DefCon4 2011–0331) for financial support. We acknowledge fruitful discussions with Viktor Kopp.

<sup>1</sup>J. Menéndez, *J. Appl. Phys.* **105**, 063519 (2009).

<sup>2</sup>*Landolt-Börnstein: Numerical Data and Functional Relationships in Science and Technology*, edited by O. Madelung, 3rd ed. (Springer-Verlag, New York, 1982), Chap. 2, pp. 3–4, 19–22, 43–68, 87–110.

- <sup>3</sup>J. Liu, X. Sun, D. Pan, X. Wang, L. C. Kimerling, T. L. Koch, and J. Michel, *Opt. Express* **15**, 11272 (2007).
- <sup>4</sup>R. E. Camacho-Aguilera, Y. Cai, N. Patel, J. T. Bessette, M. Romagnoli, L. C. Kimerling, and J. Michel, *Opt. Express* **20**, 11316 (2012).
- <sup>5</sup>L. Carroll, P. Friedli, S. Neuenschwander, H. Sigg, S. Cecchi, F. Isa, D. Chrastina, G. Isella, Y. Fedoryshyn, and J. Faist, *Phys. Rev. Lett.* **109**, 057402 (2012).
- <sup>6</sup>R. Geiger, J. Frigerio, M. J. Süess, D. Chrastina, G. Isella, R. Spolenak, J. Faist, and H. Sigg, *Appl. Phys. Lett.* **104**, 062106 (2014).
- <sup>7</sup>P. Vogl, M. M. Rieger, J. A. Majewski, and G. Abstreiter, *Phys. Scr.* **T49B**, 476 (1993).
- <sup>8</sup>O. Aldaghi, Z. Ikončić, and R. W. Kelsall, *J. Appl. Phys.* **111**, 053106 (2012).
- <sup>9</sup>R. Soref, *Nat. Photonics* **4**, 495 (2010).
- <sup>10</sup>P. Chaisakul, D. Marris-Morini, J. Frigerio, D. Chrastina, M.-S. Roufied, S. Cecchi, P. Crozat, G. Isella, and L. Vivien, *Nat. Photonics* **8**, 482 (2014).
- <sup>11</sup>P. H. Lim, S. Park, Y. Ishikawa, and K. Wada, *Opt. Express* **17**, 16358 (2009).
- <sup>12</sup>A. Ghrib, M. de Kersauson, M. El Kurdi, R. Jakomin, G. Beaudoin, S. Sauvage, G. Fishman, G. Ndong, M. Chaigneau, R. Ossikovski, I. Sagnes, and P. Boucaud, *Appl. Phys. Lett.* **100**, 201104 (2012).
- <sup>13</sup>J. Greil, A. Lugstein, C. Zeiner, G. Strasser, and E. Bertagnoli, *Nano Lett.* **12**, 6230 (2012).
- <sup>14</sup>J. R. Jain, A. Hryciw, T. M. Baer, D. A. B. Miller, M. L. Brongersma, and R. T. Howe, *Nat. Photonics* **6**, 398 (2012).
- <sup>15</sup>S. Huang, W. Lu, C. Li, W. Huang, H. Lai, and S. Chen, *Opt. Express* **21**, 640 (2013).
- <sup>16</sup>K. Tani, S. Saito, K. Oda, T. Okumura, T. Mine, and T. Ido, in *IEEE 9th Int. Conf. Group IV Photonics* (2012), pp. 328–330.
- <sup>17</sup>P. Boucaud, M. El Kurdi, S. Sauvage, M. de Kersauson, A. Ghrib, and X. Checoury, *Nat. Photonics* **7**, 162 (2013).
- <sup>18</sup>C. Boztug, J. R. Sánchez-Pérez, F. F. Sudradjat, R. B. Jacobson, D. M. Paskiewicz, M. G. Lagally, and R. Paiella, *Small* **9**, 622 (2013).
- <sup>19</sup>D. Scopece, F. Montalenti, M. Bollani, D. Chrastina, and E. Bonera, *Semicond. Sci. Technol.* **29**, 095012 (2014).
- <sup>20</sup>M. J. Süess, R. Geiger, R. A. Minamisawa, G. Schiefner, J. Frigerio, D. Chrastina, G. Isella, R. Spolenak, J. Faist, and H. Sigg, *Nat. Photonics* **7**, 466 (2013).
- <sup>21</sup>D. S. Sukhdeo, D. Nam, J.-H. Kang, M. Brongersma, and K. C. Saraswat, *Photon. Res.* **2**, A8 (2014).
- <sup>22</sup>M. Bollani, D. Chrastina, M. Fiocco, V. Mondiali, J. Frigerio, L. Gagliano, and E. Bonera, *J. Appl. Phys.* **112**, 094318 (2012).
- <sup>23</sup>E. Bonera, M. Bollani, D. Chrastina, F. Pezzoli, A. Picco, O. G. Schmidt, and D. Terziotti, *J. Appl. Phys.* **113**, 164308 (2013).
- <sup>24</sup>R. People and J. C. Bean, *Appl. Phys. Lett.* **47**, 322 (1985).
- <sup>25</sup>R. Hull, J. C. Bean, D. J. Werder, and R. E. Leibenguth, *Appl. Phys. Lett.* **52**, 1605 (1988).
- <sup>26</sup>B. W. Dodson and J. Y. Tsao, *Appl. Phys. Lett.* **53**, 2498 (1988).
- <sup>27</sup>C. G. Tuppen and C. J. Gibbings, *J. Appl. Phys.* **68**, 1526 (1990).
- <sup>28</sup>D. C. Houghton, *J. Appl. Phys.* **70**, 2136 (1991).
- <sup>29</sup>R. Beanland, *J. Appl. Phys.* **72**, 4031 (1992).
- <sup>30</sup>G. Bai, M.-A. Nicolet, C. H. Chern, and K. L. Wang, *J. Appl. Phys.* **75**, 4475 (1994).
- <sup>31</sup>G. G. Fischer and P. Zaumseil, *Phys. Status Solidi A* **164**, 767 (1997).
- <sup>32</sup>J. W. Matthews and A. E. Blakeslee, *J. Cryst. Growth* **27**, 118 (1974).
- <sup>33</sup>J. C. Bean, L. C. Feldman, A. T. Fiory, S. Nakahara, and I. K. Robinson, *J. Vac. Sci. Technol. A* **2**, 436 (1984).
- <sup>34</sup>J. G. Fiorenza, G. Braithwaite, C. W. Leitz, M. T. Currie, J. Yap, F. Singaporewala, V. K. Yang, T. A. Langdo, J. Carlin, M. Somerville, A. Lochtefeld, H. Badawi, and M. T. Bulsara, *Semicond. Sci. Technol.* **19**, L4 (2004).
- <sup>35</sup>Y. Kimura, N. Sugii, S. Kimura, K. Inui, and W. Hirasawa, *Appl. Phys. Lett.* **88**, 031912 (2006).
- <sup>36</sup>J. Parsons, E. H. C. Parker, D. R. Leadley, T. J. Grasby, and A. D. Capewell, *Appl. Phys. Lett.* **91**, 063127 (2007).
- <sup>37</sup>J. M. Hartmann, A. Abbadie, Y. Guinche, P. Holliger, G. Rolland, M. Buisson, C. Defranoux, F. Pierrel, and T. Billon, *Semicond. Sci. Technol.* **22**, 354 (2007).
- <sup>38</sup>J. M. Hartmann, A. Abbadie, D. Rouchon, M. Mermoux, and T. Billon, *Semicond. Sci. Technol.* **22**, 362 (2007).
- <sup>39</sup>J. M. Hartmann, A. Abbadie, D. Rouchon, J. P. Barnes, M. Mermoux, and T. Billon, *Thin Solid Films* **516**, 4238 (2008).
- <sup>40</sup>L. H. Wong, J. P. Liu, C. C. Wong, C. Ferraris, T. J. White, L. Chan, D. K. Sohn, and L. C. Hsia, *Electrochem. Solid State* **9**, G114 (2006).
- <sup>41</sup>B. Bertoli, E. N. Suarez, F. C. Jain, and J. E. Ayers, *Semicond. Sci. Technol.* **24**, 125006 (2009).
- <sup>42</sup>V. A. Shah, A. Dobbie, M. Myronov, and D. R. Leadley, *J. Appl. Phys.* **107**, 064304 (2010).
- <sup>43</sup>A. Dobbie, V. H. Nguyen, R. J. H. Morris, X.-C. Liu, M. Myronov, and D. R. Leadley, *J. Electrochem. Soc.* **159**, H490 (2012).
- <sup>44</sup>B. G. Demczyk, V. M. Naik, S. Hameed, and R. Naik, *Mater. Sci. Eng. B* **94**, 196 (2002).
- <sup>45</sup>G. Capellini, M. De Seta, Y. Busby, M. Pea, F. Evangelisti, G. Nicotra, C. Spinella, M. Nardone, and C. Ferrari, *J. Appl. Phys.* **107**, 063504 (2010).
- <sup>46</sup>J. Osmond, G. Isella, D. Chrastina, R. Kaufmann, M. Acciarri, and H. von Känel, *Appl. Phys. Lett.* **94**, 201106 (2009).
- <sup>47</sup>V. S. Kopp, V. M. Kaganer, G. Capellini, M. De Seta, and P. Zaumseil, *Phys. Rev. B* **85**, 245311 (2012).
- <sup>48</sup>P.-Y. Hsiao, Z.-H. Tsai, J.-H. Huang, and G.-P. Yu, *Phys. Rev. B* **79**, 155414 (2009).
- <sup>49</sup>T. J. Gosling, S. C. Jain, and A. H. Harker, *Phys. State Solidi A* **146**, 713 (1994).
- <sup>50</sup>J. P. Dismukes, L. Ekstrom, and R. J. Paff, *J. Phys. Chem.* **68**, 3021 (1964).
- <sup>51</sup>J. J. Wortman and R. A. Evans, *J. Appl. Phys.* **36**, 153 (1965).
- <sup>52</sup>A. Marzegalli, F. Montalenti, M. Bollani, L. Miglio, G. Isella, D. Chrastina, and H. von Känel, *Microelectron. Eng.* **76**, 290 (2004).
- <sup>53</sup>J. Parsons, C. S. Beer, D. R. Leadley, A. D. Capewell, and T. J. Grasby, *Thin Solid Films* **517**, 17 (2008).
- <sup>54</sup>L. B. Freund, *J. Appl. Phys.* **68**, 2073 (1990).
- <sup>55</sup>V. T. Gillard, W. D. Nix, and L. B. Freund, *J. Appl. Phys.* **76**, 7280 (1994).
- <sup>56</sup>M. Bonfanti, E. Grilli, M. Guzzi, M. Virgilio, G. Grosso, D. Chrastina, G. Isella, H. von Känel, and A. Neels, *Phys. Rev. B* **78**, 041407(R) (2008).